

# TRAFFIC SIGNAL CONTROL ALGORITHM BASED ON QUEUING MODEL USING ITS SENSING TECHNOLOGIES

Miho Asano<sup>1)</sup>, Akira Nakajima<sup>2)</sup>, Ryota Horiguchi<sup>3)</sup>,  
Hiroyuki Oneyama<sup>4)</sup> and Masao Kuwahara<sup>5)</sup>

1) Institute of Industrial Science, The University of Tokyo  
Cw-504, 4-6-1 Komaba, Meguro-ku, Tokyo 153-8505, Japan  
Tel: +81 3 5452 6419 - Fax: +81 3 5452 6420 e-mail: asano@nishi.iis.u-tokyo.ac.jp

2) Institute of Industrial Science, The University of Tokyo  
e-mail: nkjm@sak.iis.u-tokyo.ac.jp

3) i - transport lab, 2-12-404 Ageba-cho, Shinjuku-ku, Tokyo 162-0824, Japan  
e-mail: horiguchi@i-transportlab.jp

4) National Institute for Land and Infrastructure Management,  
1 Asahi, Tsukuba-shi, Ibaraki 305-0804, Japan  
e-mail: oneyama-h92bi@nilim.go.jp

5) Institute of Industrial Science, The University of Tokyo  
e-mail: kuwahara@nishi.iis.u-tokyo.ac.jp

## SUMMARY

This study has developed a new traffic signal control algorithm with ITS sensing technologies. These technologies can measure the travel time of individual vehicle, so this algorithm can evaluate delay and search the optimal combination of signal parameters to minimize the total delay in a network, based on a queuing model. We examined the effect of this algorithm with simulation experiment and plan to implement it as a real-world system for a demonstration in the next ITS World Congress in Nagoya, 2004.

## INTRODUCTION

The purpose of this research is to develop a new traffic signal control algorithm that can minimize total delay directly measured by Intelligent Transport Systems (ITS) sensing technologies.

Technologies of traffic sensing and communications have been developing rapidly by the progress of ITS. We may expect that the technology to identify individual vehicles by image processing or uplink from floating cars will be much facilitated in near future. These technologies allow us to directly measure the travel time of individual vehicle in a desired section, which has not been utilized in the conventional signal control methods such as SCOOT or SCAT.

The algorithm proposed here uses the travel time of each vehicle in order to calculate total delay of each approaching link at a signalised intersection<sup>(1)</sup>. For each cycle of a signalised intersection, the algorithm updates signal parameters, i.e. split, cycle and offset, in terms of the improvement on delay at the intersection. As the changes on parameters are discretized into sufficiently small unit, e.g. 2 or 3 seconds, and are limited one or two units at maximum, the algorithm can find the optimal parameter set by solving combinational optimisation

problem. In order to reduce the calculation cost, the algorithm assumes ‘common cycle length’ to be shared in the signalised intersection in a “sub-area”, which normally consists of several intersections.

The most remarkable feature of this algorithm is adaptation. Most of the conventional signal control methods would have some key parameters that greatly affect performance. For instance, the program selection control used in Japan has pre-determined sets of signal parameters, which should be carefully calibrated to achieve better performance, and selects appropriate parameters for the traffic condition at the moment. However, after a long-run, traffic situation may be different from those for which traffic signal was calibrated, and the program selection control may not work well without continuous maintenance. In this algorithm, all key parameters are directly measured and updated at every cycle, therefore the algorithm can maintain the expected performance for a long time.

We have a plan to implement the algorithm proposed here to a real-world system. In this experiment, AVI (Automatic Vehicle Identification) sensors are used by taking into account practical use of the algorithm, but we may expect to use cheaper sensors based on a technology of tracing vehicle trajectories by image processing in the future<sup>(2)</sup>. As a demonstration at the next ITS World Congress in Nagoya, 2004, the system will be operated for the Nagoya-Nagakute road, which is also test bed for this experiment.

In the following chapters, we will explain how to estimate the delay from the arrival-departure cumulative flow diagrams (called as “cumulative curves” in this paper) and how the controlling algorithm proposed here will modify signal parameters cycle by cycle. The last part of this paper will report the performance of the algorithm through computational experiments with traffic simulation.

## DELAY ESTIMATION OVER A LINK

### Data requirements and arrangement of sensors

The algorithm requires two kinds of information to figure out the cumulative curve for a subjective link; i.e. the time profile of vehicle counts of departure traffic from the intersection and the travel times of individual vehicles over the link. Especially for departure vehicle counts, data of all the vehicles are required to know the amount of traffic flow. In order to obtain those information, we are using two types of sensors, ultrasonic detector and AVI sensor, which are currently installed at the road in Japan. AVI sensors can measure the travel time of each vehicle, and ultrasonic detectors can provide the profile of vehicle counts more accurately than AVI sensors.

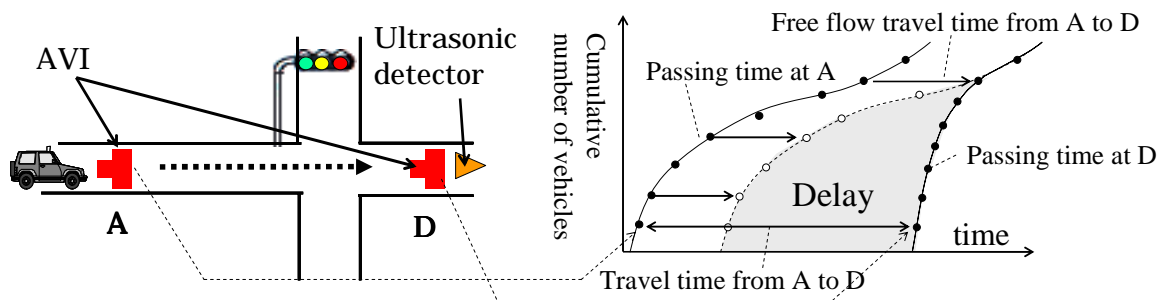


**Figure 1 Cumulative curves to estimate delay and arrangement of sensors**

The required arrangement of sensors is shown as Figure 1. To exclude the influence of the queue extended from the downstream intersection, these detectors are put the upstream of each link. AVIs are set on both point A and D. Data obtained from AVI is the passing time and ID number of each vehicle. Matched by the ID numbers between two points, the travel time of the vehicles can be measured. Ultrasonic detectors are put on point D to get the number of vehicles which passed the intersection.

### Drawing cumulative curves from the observed data

This algorithm measures the delay to optimize signal parameters using cumulative curves. The cumulative curves of vehicles which passed the point A and D are drawn as right part of Figure 1. The horizontal distance between these curves shows the travel time from A to D of each vehicle. If the curve of passing time at A is shifted to right as much as the free flow travel time from A to D, the delay caused by signal controller can be estimated as the gray-colored area.

The throughput volume at the upstream end of each out-flow link of an intersection is measured by ultrasonic detector. Synchronizing the cumulative throughput with the signal phase of the intersection, the cumulative departure curve of each approach can be obtained (the D-curve in Figure 2).

Then, cumulative arrival curves of each approach of an intersection are estimated. Suppose each link in the subjective area has the AVI sensors to identify individual vehicle at its upstream end as shown in Figure 1, the travel time of a sample vehicle can be measured over the link. By subtracting the free flow travel time of the link, the delay of an identified vehicle is obtained.

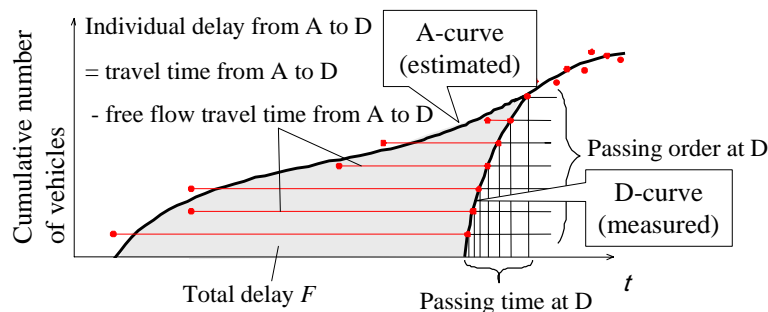


**Figure 2 Cumulative curves**

As shown in Figure 2, the arrival time of each identified vehicle can be estimated by shifting corresponding point on D-curve to the left (= past) as much as the delay of the vehicle. Since First In First Out (FIFO) principle is not always kept in the real world, the estimated arrival points of identified vehicles are to be sorted by time, and we estimate the cumulative arrival curve (A-curve) by interpolating those arrival points. The total delay per cycle  $F$  at this stream is represented as the sum of the delay of each vehicle, which means the area enclosed by A-curve and D-curve.

The free flow travel time of each links is estimated in order to take out the delay from travel time. From the AVI data, the travel time of each vehicle from point A to point D in Figure 1 can be measured. The histogram of the travel time in Figure 3 can be divided into two parts; one shows travel times of vehicles which can pass this link without stopping, and the other shows the travel times of vehicles which stop by red light. The free flow travel time  $T_F$  is determined as the mode of the vehicles which can pass this link without stopping. The difference between travel time and free flow travel time is the delay caused by traffic signals.

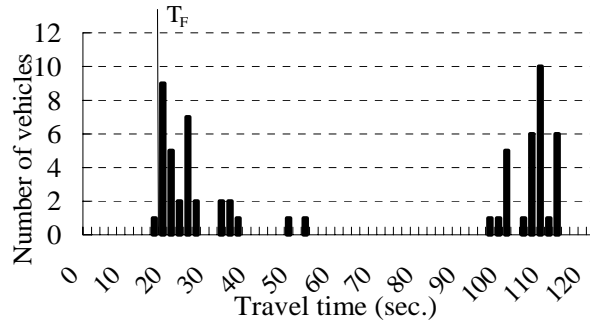


Figure 3 An example of Travel time statistics to estimate  $T_F$

## PARAMETER MODIFICATION TO MINIMIZE DELAY

### Outlines of parameter modification

In this chapter, the signal parameters to minimize the total delay will be determined. Now we will represent the splits and offsets in second in this paper while they are usually represented as the percentage of cycle time.

In this algorithm, changes on parameters are discretized by small intervals. We search the parameters from the neighbourhood of the present parameter set, estimating the change on delay in each case. It is result in combinational search of the signal control parameters; split and cycle times of each intersection and offsets of each link. The intervals of each parameter are  $\Delta_s$ ,  $\Delta_c$  and  $\Delta_o$ . We have 3 patterns to choose split of one intersection, and same as offset and cycle times, which are the cases that parameter increases, decreases and keeps the present value. However, the number of choice set is too large to search at this time. To reduce the number of combination, we have some assumptions.

The first assumption is that the traffic conditions in the next cycle will be the same as in the latest cycle. This assumption makes us possible to use the cumulative curves drawn in the previous chapter as the curve of the next cycle if the signal parameters keep the same value as the latest cycle. The changes on delay when signal parameters change are estimated using the cumulative curves of the latest cycle.

The second, third and fourth assumptions are to reduce the number of combination of search area. The second is that we consider a group of intersections which share the common cycle time. The group is called as “sub-area” in this paper.

The third is that the search of offset is done only when the common cycle time keeps the present value. That’s because the offsets naturally change when cycle time changes and so we only consider the influence of changes on offset caused by change of cycle time.

According to the third assumption, the change of offset with cycle increase can be decided. Here, we only consider ‘positive’ offset values; i.e. when the offset of one direction is  $x$  [sec.], the other direction must be  $(C-x)$  [sec.], where  $C$  is a cycle length. Suppose the common cycle length will be increased by  $\Delta_c$  as shown in Figure 4, the offset values will be  $x$  and  $(C-x + \Delta_c)$ , if they are untouched. However, it is quite unfair to impose a burden on one direction. Therefore, the changes on offset will be shared for both directions as  $(x/C) \Delta_c$  and  $((C-x)/C) \Delta_c$ . Remember the sum of both changes must be always  $\Delta_c$ .

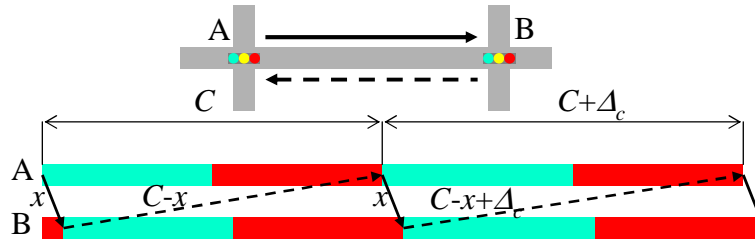


**Figure 4** Changes on ‘positive’ offset values when the cycle length changes

The fourth assumption is that the splits are decided first, with no relation to change on offsets and cycle time. Offsets and cycle time will be determined after choosing splits.

For instance, suppose there is a network consists of  $N$  intersections and  $N-1$  links. Since the parameters can take 3 patterns; no change, increase and decrease, the number of parameter combination is  $3^{3N-1}$ . If the whole network is considered as one sub-area, the number of combination with these assumptions can be reduced to  $4 * 3^{N-1} + 2$ .

### Estimation of changes in delay

Applying the first assumption, we may evaluate the improvement on the delay of each stream when the signal parameters change. Figure 5 explains that the case when the split of one green phase of an intersection changes by  $\pm\Delta_s$ . The shape of arrival and departure curves were borrowed from the latest observation. If the split increases  $\Delta_s$  to the current value, the D-curve will shift to the upper dotted line, because the green phase of the next cycle starts with the lag  $\Delta_s$ .

The case when the offset of a link changes by  $\pm\Delta_o$  is similar to this. The estimated curves are shown in Figure 6. Since the number of combination of the changes on split and offset is  $3 \times 3$ , the  $3 \times 3$  types of the curves and the changes on delay are estimated. The changes on delay

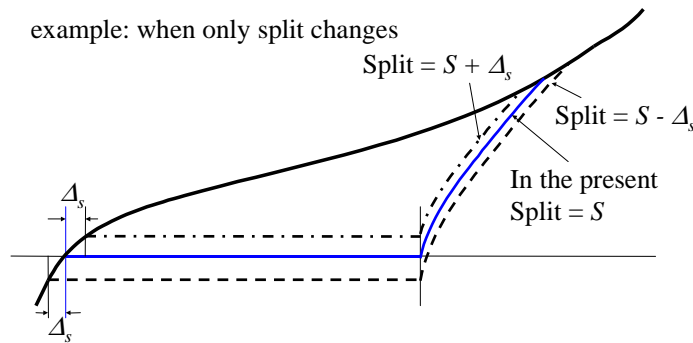


**Figure 5** Estimating the changes on delay when split  $S$  is modified

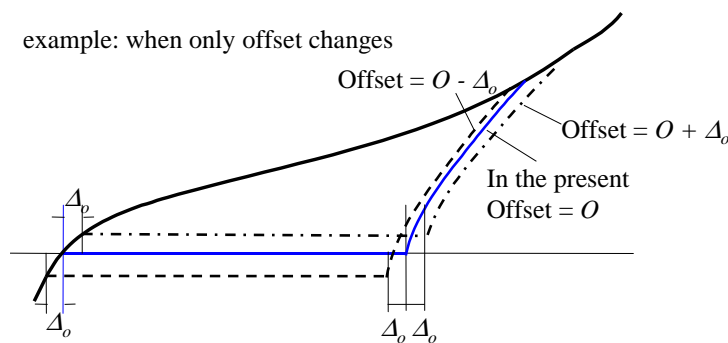


**Figure 6** Estimating the changes on delay when offset  $O$  is modified

**Table 1 Matrix of changes on delay by the change of split and offset**

		Change of offset		
		-	0	+
Change of split	-	$\left(\frac{\partial F}{\partial s^-}, \frac{\partial F}{\partial o^-}\right)$	$\left(\frac{\partial F}{\partial s^-}, 0\right)$	$\left(\frac{\partial F}{\partial s^+}, \frac{\partial F}{\partial o^-}\right)$
	0	$\left(0, \frac{\partial F}{\partial o^-}\right)$	0	$\left(0, \frac{\partial F}{\partial o^+}\right)$
	+	$\left(\frac{\partial F}{\partial s^-}, \frac{\partial F}{\partial o^+}\right)$	$\left(\frac{\partial F}{\partial s^+}, 0\right)$	$\left(\frac{\partial F}{\partial s^+}, \frac{\partial F}{\partial o^+}\right)$

of each stream can be formed as a matrix like Table 1. Here,  $F$  is the total delay of the latest cycle at this stream. This table shows, for instance, the estimated value of the change on delay when the split and offset increase  $\Delta_s$  and  $\Delta_s$  is represented as  $\left(\frac{\partial F}{\partial s^+}, \frac{\partial F}{\partial o^+}\right) \cdot \begin{pmatrix} \Delta_s \\ \Delta_o \end{pmatrix}$ , where  $\left(\frac{\partial F}{\partial s^+}, \frac{\partial F}{\partial o^+}\right)$  is put in the cells that both row and column are “+”. From the matrices of each stream, the parameters to minimize the total delay of the sub-area are decided.

## Modification of parameters without changing common cycle length

### Modification of splits

Assume that the offsets and the common cycle time do not change. In the case that the split of Stream 1 and 3 in Figure 7 is increased, the change of the delay at this intersection is the sum of the  $\left(\frac{\partial F}{\partial s^+}, 0\right) \cdot \begin{pmatrix} \Delta_s \\ 0 \end{pmatrix}$  of Stream 1 and 3 and of the  $\left(\frac{\partial F}{\partial s^-}, 0\right) \cdot \begin{pmatrix} -\Delta_s \\ 0 \end{pmatrix}$  of Stream 2 and 4. The opposite is in the case that the split of Stream 1 and 3 is decreased. If the split doesn't change, the change on delay is equal to 0. Split is chosen from these 3 cases which minimize the delay of the intersection.

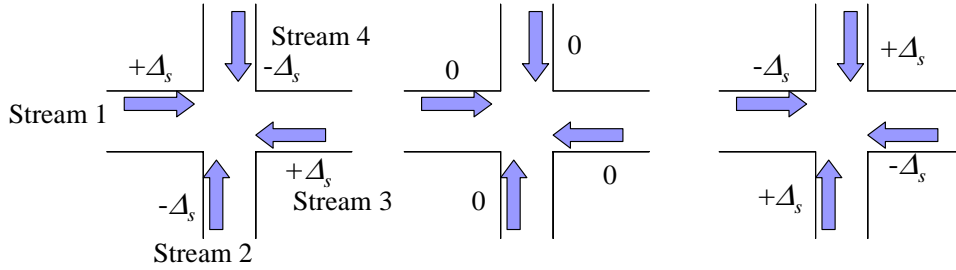


**Figure 7 Three patterns of split change at an intersection**

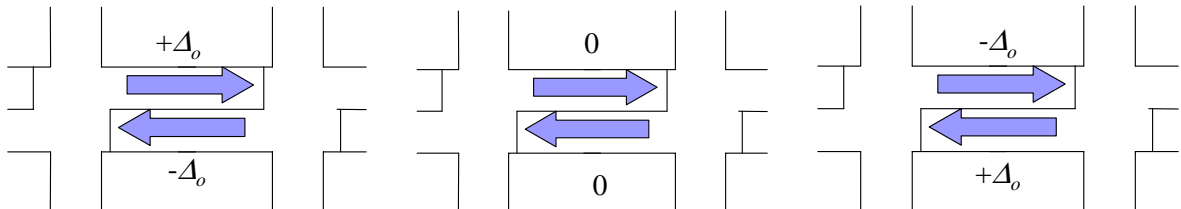


**Figure 8 Three patterns of offset change at a link**

### Modification of offsets

For each link, there are 3 patterns to be chosen as Figure 8; offset to east increases or decreases, and offset doesn't change. In this case, change on split in each intersection is

obtained from the previous process, modification of splits. From the matrices of changes on delay, choose one pattern to minimize the delay in the link.

## Modification of parameters with changing common cycle length

### Modification of splits

The way of modification of split is exactly the same as in the case without changing common cycle time.

### Modification of offsets and common cycle time

#### (1) Basic change on delay

Offset and common cycle time are decided simultaneously. Suppose the subjective intersection and the upstream intersection share the same cycle time. The shape of the arrival curve of the subjective stream is affected by the shape of the departure curve at the upstream intersection. Since the departure curve at the upstream intersection may change by changing the cycle time, we assume that the arrival curve at subjective intersection will also change in accordance with change in departure curve of upstream intersection, as common cycle time changes by  $\Delta_c$  as shown in Figure 9. In Figure 9,  $G$ ,  $R$  and  $L$  show the effective green length of the subjective stream, sum of the effective green length of other streams and loss time of the intersection respectively. If departure curve at subjective intersection also changes similar to the arrival, the changes on delay in the whole sub-area per unit time are shown as follows.

$$\sum_i \left( F_i \cdot \left( \frac{C + \Delta_c}{C} \right)^2 \cdot \frac{1}{C + \Delta_c} - F_i \cdot \frac{1}{C} \right) = \sum_i \frac{F_i \Delta_c}{C^2} \quad (Eq. 1)$$

Here,  $F_i$  is the total delay in stream  $i$  per cycle.

In fact, departure curves don't change exactly similarly. There are three properties which correct the departure curve. The first is "*correction of offset*" which occurs because of the changes on offsets as the common cycle time changes. The second property is "*correction of loss time*" which occurs because the loss time does not change with cycle time. The last one is "*correction of saturation flow rate decline.*" If the cycle time gets larger, it is known that saturation flow rate may decline at a certain point because the right turners spill over the exclusive right turn lane and block another lane, or because queue from the downstream may reach the intersection.

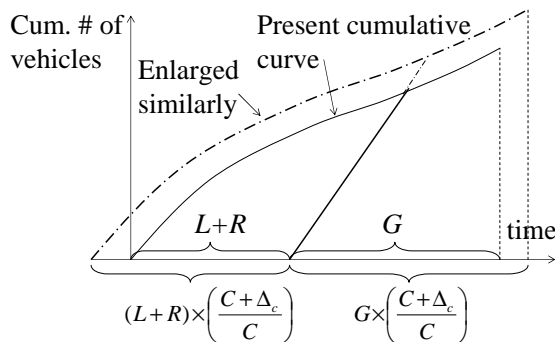


**Figure 9** Enlarged cumulative curves as common cycle time increases

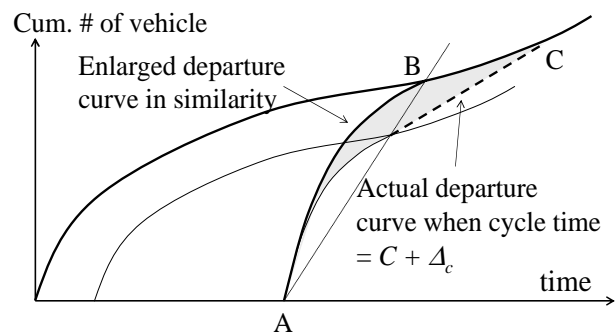


**Figure 10** Correction of saturation flow rate decline

#### (2) Correction of offset and loss time

Consider the difference of delay between the basic curve and the curve which corrected taking into account of the property of offset and loss time. Since the loss time is constant, the green

length does not change similarly by cycle. Moreover, the offset changes by  $\frac{x}{C}\Delta_c$  from the assumption. Combining these properties, the correction of offset and loss time is obtained. The proof is in the appendix.

$$Cor_{o_i}^+ = \sum_i \sum_j \left( \left( \frac{\partial F}{\partial s^+}, \frac{\partial F}{\partial o^+} \right) \begin{pmatrix} \Delta_s \\ \Delta_o \end{pmatrix} \right)_j \cdot \frac{\Delta_c (C + \Delta_c)}{2C^2} \left( \frac{GL}{(C-L)\Delta_s} + \frac{x}{\Delta_o} \right) \quad (Eq. 2)$$

Where  $i$  and  $j$  show the  $j$  th stream at  $i$  th intersection.

### (3) Correction of saturation flow rate decline

When departure curve is enlarged similarly, the curve will be drawn as AB in Figure 10. However, the actual departure curve is drawn as AC, because the saturation flow rate may decrease as the green length gets longer. The gray area in Figure 10 should be the correction of saturation flow rate decline.

## Choice of the best parameter set

Now the combination of signal parameters which best decreases the total delay in the whole sub-area is chosen. At first, splits of each intersection are decided. The total change on delay caused by change on offset and common cycle time is obtained as follows.

In the case without changing cycle time, the total change on delay is the sum of the change on delay of each link whose parameters are chosen to minimize the delay. In the case with changing cycle time, the total changes on delay are expediently represented as the sum of the basic changes and corrections of each stream. Comparing these three cases of no change, increase and decrease, the combination of common cycle time and offsets that minimize the total delay is chosen as the parameter of the next cycle.

## APPLICATION USING TRAFFIC SIMULATION “AVENUE”

### Study Area

The performance of this algorithm is examined using the traffic simulation model AVENUE<sup>(3)</sup>. The study network is selected along the Nagakute line in the Nagoya central district. The network has a tree shape and consists of 10 links and 11 intersections. The places of the sensors are shown in Figure 11. We basically referred to the actual place of sensors and added sensors on the arterial road if they are not in the link. The delays of the minor road without any sensors are regarded as 0.

The simulation time is 2 hours and 10 minutes. The first 10 min. is used for warming up the simulation to distribute vehicles throughout the study area, and after that the algorithm started. We have three cases to examine whether parameters can follow the change of traffic demand. In case 1 the degrees of saturation of intersections stay between 0.5-0.7, and 0.5-0.95 in case 2 as shown in Figure 12. In case 3, the degrees of saturation are the same as case 1, and the saturation flow rate decreases 20% in the latter half of the simulation time. The initialization values of signal control parameters are as follows. Common cycle time is 120 sec, and splits of arterial road are set between 53% and 62%. The offset of every link are set to 0%.

In this experiment,  $\Delta_c$  is set as 4 sec, and  $\Delta_s$  and  $\Delta_o$  are set as 2 sec. As restrictions, the allowable range of the common cycle time is between 80 and 160 sec, and the minimum



green lengths of each stream are 30 sec. We regarded the whole study area as one sub-area. The simulation results are evaluated in terms of total delay of each intersection and history of the signal parameters as evaluation indices.

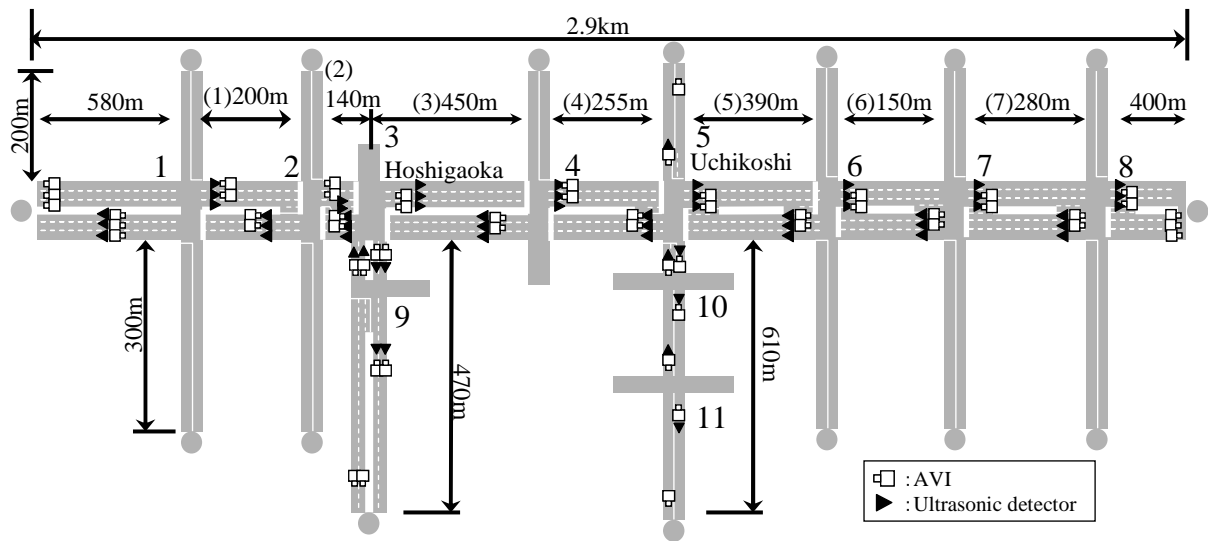


Figure 11 The study network along the Nagakute line, Nagoya

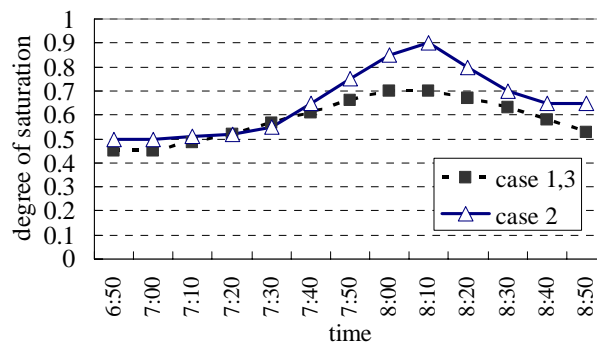


Figure 12 Degree of saturation at Uchikoshi intersection

## Results of the simulation experiment

### Total delay

Figure 13- 15 show the total delay of the major road in the whole area and of the minor road at Uchikoshi and Hoshigaoka intersection in each case. In those figures, “without algorithm” means the case that the signal parameters keep the initialization value in the whole simulation.

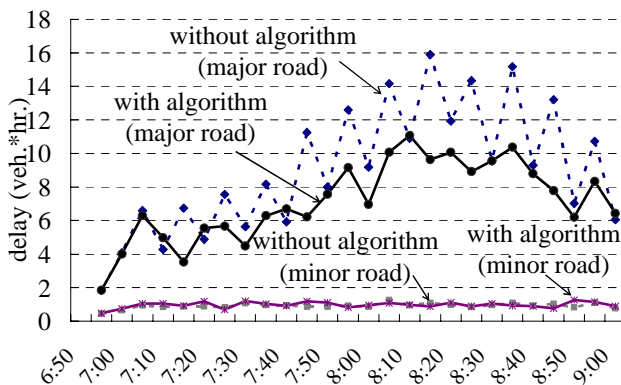


Figure 13 Total delay in the Case 1

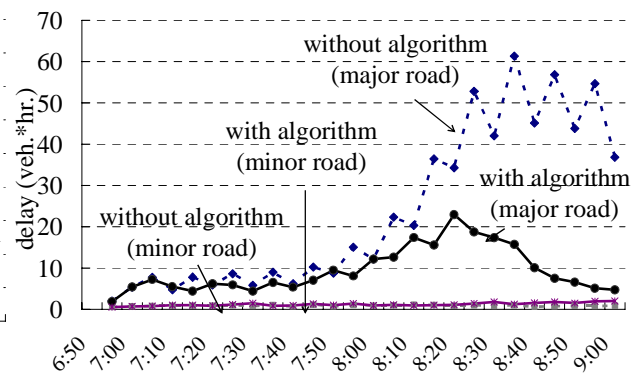
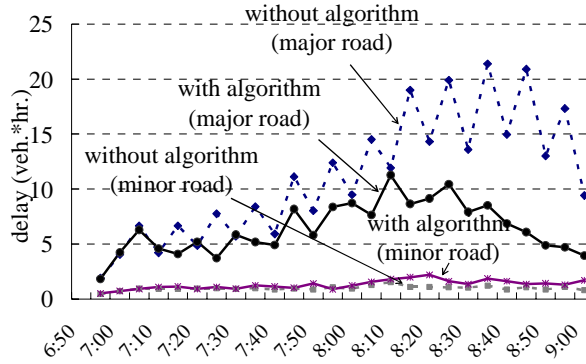


Figure 14 Total delay in the Case 2



**Figure 15 Total delay in the Case 3**

Here, the delays decrease in every case. Especially in the case 3 (Figure 15), although the delay without this algorithm increases compared to the case 1, the delay is almost the same as the case 1 with the system. It follows from this that the algorithm can control considering the decrease of the saturation flow rate by measuring not only the arrival flow but also the departure flow.

Signal parameters

Figure 16 - 21 show the changes on signal parameters in each case. The offset means the offset to the east. In Figure 16, the cycle time gradually decreases in spite of demand change. It suggests that the initialization value of the cycle time was too large. It also appears that cycle time swings in every cycle. This is because the parameters are affected by the randomness of demand, and because cycle time is required to modify to update the offsets.

In the case 2 and 3, the cycle time increases even after the traffic demand decreased. That is because the queue occurs even if the cycle time increases to the maximum value.

There are some links whose offset constantly increases / decreases. The reason is that  $\Delta_o$  is not enough large to be settled in the simulation time. To apply this algorithm to actual field, it is better that the initialization value of offset needs to be near the optimum value to some extent or that  $\Delta_s$ ,  $\Delta_o$  and  $\Delta_c$  should increase to follow the traffic condition earlier.

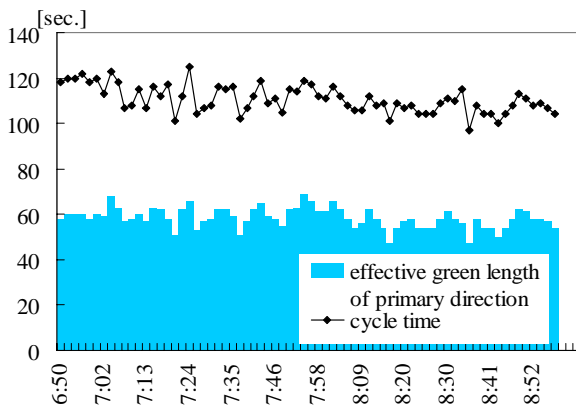


**Figure 16 Cycle time and green time length of the main direction at Uchikoshi intersection in the Case 1**

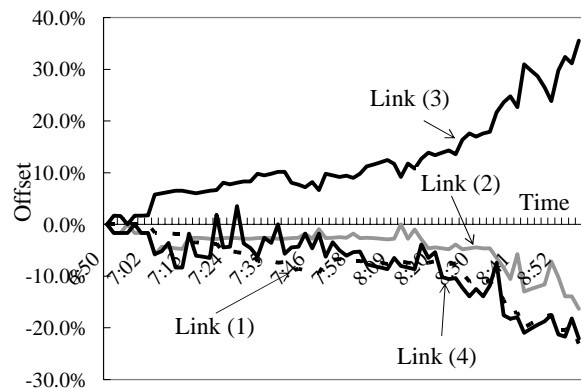


**Figure 17 Offset of each link in the Case 1**

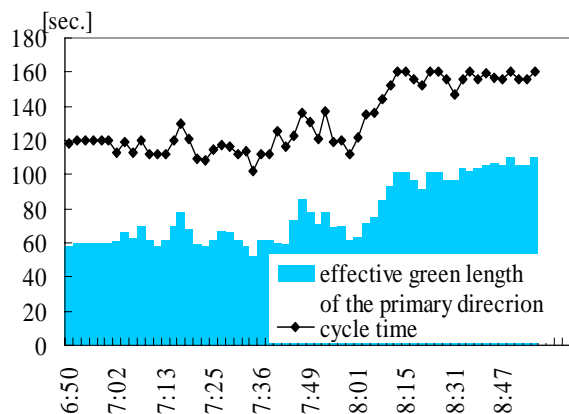


Figure 18 Cycle time and green time length of the main direction at Uchikoshi intersection in the Case 2

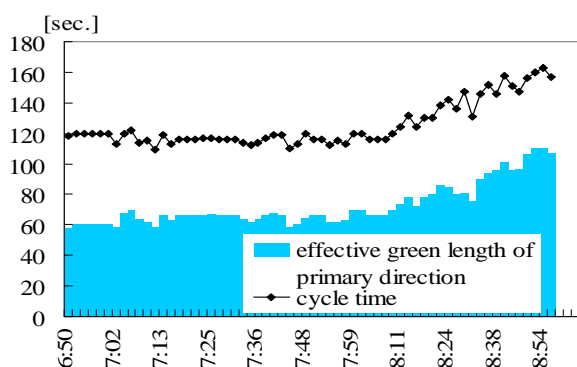


Figure 20 Cycle time and green time length of the main direction at Uchikoshi intersection in the Case 3

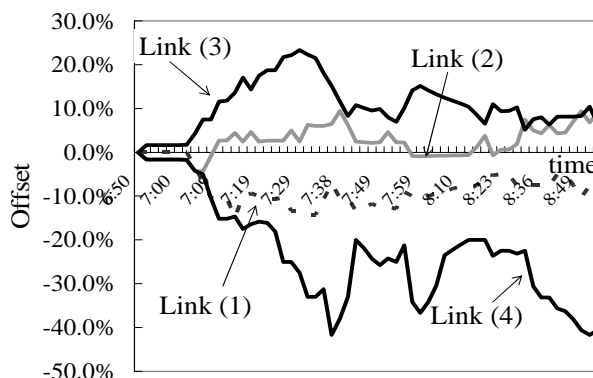


Figure 19 Offset of each link in the Case 2

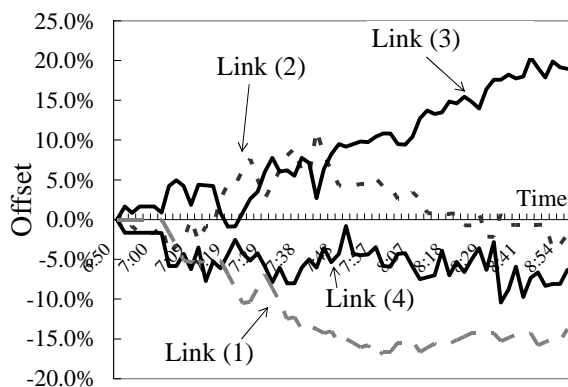


Figure 21 Offset of each link in the Case 3

## CONCLUSIONS

This study has developed a signal control algorithm based on a traffic model that can directly evaluate total delay measured by sensors. The result of the simulation experiment shows that this algorithm can really reduce the delay of the whole network in each case without any parameter tuning.

For future study, we plan to add an optimization system for case of saturated traffic condition. To follow the traffic condition earlier, we will improve the system applying the forecast of arrival flow. Now we are discussing for practical use through field experiment at this network. We are also planning to have a demonstration of this system in ITS World Congress in Nagoya, 2004.

## REFERENCES

- (1) M. Koshi, *et al.*; "A Traffic Signal Algorithm using ITS Sensing Technologies", *Proceedings of Infrastructure Planning*, Vol.25, 2002 (in Japanese)
- (2) S. Kamijo, *et al.*; "Occlusion Robust and Illumination Invariant Vehicle Tracking for Acquiring Detailed Statics from Traffic Images", *IEICE Trans. on Information and System*, Vol. E-85-D, No.11, November 2002

- (3) R. Horiguchi, *et al.*; “A Network Simulation Model for Impact Studies of Traffic Management ‘AVENUE Ver.2’ ”, *Proceedings of the Third Annual World Congress on Intelligent Transport Systems*, ITS America, 1996

## APPENDIX---CORRECTION OF OFFSET AND LOSS TIME

Vector  $\phi = \{s, o\}$  is defined in which  $s$  is the split and  $o$  is the offset of the subjective stream.

$$\nabla F = \left( \frac{\partial F}{\partial s}, \frac{\partial F}{\partial o} \right), \quad \nabla F' = \left( \frac{\partial F'}{\partial s}, \frac{\partial F'}{\partial o} \right) \quad (\text{Eq. 3})$$

$F'$  is the delay of the curve which is enlarged similarly by  $(C + \Delta_c) / C$ .

Because of the similarity assumption,

$$\frac{\partial F'}{\partial s} = A \frac{\partial F}{\partial s}, \quad \frac{\partial F'}{\partial o} = A \frac{\partial F}{\partial o} \quad \therefore \nabla F' = \nabla F \cdot A \quad \text{where } A = \frac{C + \Delta_c}{C} \quad (\text{Eq. 4})$$

If the curve is simply enlarged, the green length would be  $\frac{C + \Delta_c}{C} G$ . However, the actual

green length is  $\frac{C + \Delta_c - L}{C - L} G$  because the loss time is independent of cycle. The correction value of split  $\Delta_s'$  is

$$\Delta_s' = \left( \frac{C + \Delta_c - L}{C - L} - \frac{C + \Delta_c}{C} \right) G = \frac{GL\Delta_c}{C(C - L)} \quad (\text{Eq. 5})$$

Then the cumulative departure curve should be shifted like Figure 22. The gray-colored area is shown as the correction of loss time.

The actual change on offset  $\Delta_o'$  is  $\frac{x}{C} \Delta_c$  from the assumption.

Therefore, the correction of offset and loss time of one stream per cycle is shown as following equation, using  $\Delta'_\phi = (\Delta_s', \Delta_o')$ .

$$\nabla F' \cdot \Delta'_\phi = A \nabla F \Delta_\phi \Delta_\phi^{-1} \Delta'_\phi = \nabla F \Delta_\phi \cdot \frac{(C + \Delta_c) \Delta_c}{C^2 (\Delta_s^2 + \Delta_o^2)} \left( \frac{GL\Delta_s}{(C - L)} + x\Delta_o \right) \quad (\text{Eq. 6})$$

Finally, the correction of offset and loss time of whole the sub-area per unit time in the case of increase of the cycle time is obtained.

$$Cor_{o-t}^+ = \sum_i \sum_j \left( \left( \frac{\partial F}{\partial s^+}, \frac{\partial F}{\partial o^+} \right) \left( \Delta_s \right) \right)_j \cdot \frac{\Delta_c}{C^2 (\Delta_s^2 + \Delta_o^2)} \left( \frac{GL\Delta_s}{(C - L)} + x\Delta_o \right) \quad (\text{Eq. 7})$$

Where  $i$  and  $j$  show the  $j$  th stream at  $i$  th intersection.

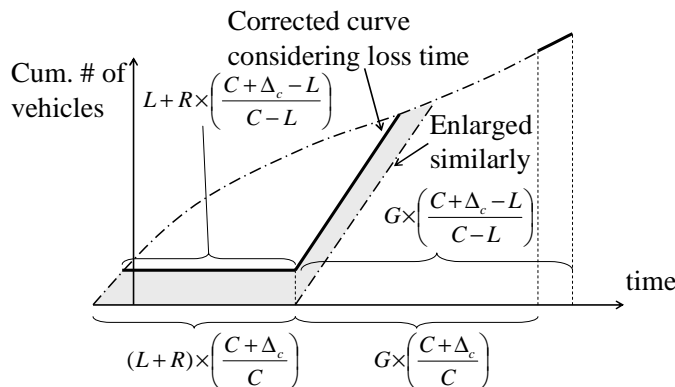


Figure 22 Correction of loss time